



Published in final edited form as:

Cell Metab. 2013 January 8; 17(1): 49–60. doi:10.1016/j.cmet.2012.12.011.

Trimethylamine-N-Oxide, a Metabolite Associated with Atherosclerosis, Exhibits Complex Genetic and Dietary Regulation

Brian J. Bennett^{1,2,**,#}, Thomas Q. de Aguiar Vallim^{1,3,#}, Zeneng Wang^{4,#}, Diana M. Shih¹, Yonghong Meng¹, Jill Gregory⁴, Hooman Allayee⁵, Richard Lee⁶, Mark Graham⁶, Rosanne Crooke⁶, Peter A. Edwards^{1,3}, Stanley L. Hazen⁴, and Aldons J. Lusis^{1,2,7}

¹Department of Medicine, University of California, Los Angeles

²Department of Human Genetics, University of California, Los Angeles

³Department of Biological Chemistry, University of California, Los Angeles

⁴Department of Cellular & Molecular Medicine, Center for Cardiovascular Diagnostics & Prevention and Department of Cardiovascular Medicine, Cleveland Clinic, Cleveland, OH 44195

⁵Department of Preventive Medicine and Institute for Genetic Medicine, USC Keck School of Medicine, Los Angeles, CA 90089-9075

⁶ISIS Pharmaceuticals, 2855 Gazelle Court, Carlsbad, CA 92010

⁷Department of Microbiology, Immunology and Molecular Genetics, University of California, Los Angeles, CA 90095

SUMMARY

Circulating trimethylamine-N-oxide (TMAO) levels are strongly associated with atherosclerosis. We now examine genetic, dietary, and hormonal factors regulating TMAO levels. We demonstrate that two flavin monooxygenase family members, FMO1 and FMO3, oxidize trimethylamine (TMA), derived from gut flora metabolism of choline, to TMAO. Further, we show that FMO3 exhibits 10-fold higher specific activity than FMO1. FMO3 overexpression in mice significantly increases plasma TMAO levels while silencing FMO3 decreases TMAO levels. In both humans and mice, hepatic FMO3 expression is reduced in males compared to females. In mice, this reduction in FMO3 expression is due primarily to down-regulation by androgens. FMO3 expression is induced by dietary bile acids by a mechanism that involves the farnesoid X receptor (FXR), a bile acid-activated nuclear receptor. Analysis of natural genetic variation among inbred strains of mice indicates that FMO3 and TMAO are significantly correlated, and TMAO levels explains 11% of the variation in atherosclerosis.

© 2012 Elsevier Inc. All rights reserved.

Correspondence to: Brian J. Bennett, Department Genetics, Nutrition Research Institute, 500 Laureate Way Suite 2303, Kannapolis, NC 28081, Or Aldons J. Lusis, Department of Medicine/Division of Cardiology, A2-237 Center for the Health Sciences, UCLA School of Medicine, University of California, Los Angeles, CA 90095-1679.

** Present address:

Department of Genetics, University of North Carolina, Chapel Hill, NC
Nutrition Research Institute, University of North Carolina, Kannapolis, NC

Authors contributed equally to this manuscript

Publisher's Disclaimer: This is a PDF file of an unedited manuscript that has been accepted for publication. As a service to our customers we are providing this early version of the manuscript. The manuscript will undergo copyediting, typesetting, and review of the resulting proof before it is published in its final citable form. Please note that during the production process errors may be discovered which could affect the content, and all legal disclaimers that apply to the journal pertain.

INTRODUCTION

Recently, plasma trimethylamine-N-oxide (TMAO) was identified as a metabolite strongly associated with atherosclerosis in a large case-control cohort for cardiovascular disease (CVD) and studies in mice indicated a causal relationship (Wang et al., 2011). TMAO is derived from dietary choline through the action of gut flora, which metabolize choline to trimethylamine (TMA), a gas that is then absorbed into the circulation and further metabolized to TMAO. Likely candidates for the conversion of TMA to TMAO are members of the flavin monooxygenase (FMO) family. In particular, FMO3 has been implicated in the oxidation of TMA since individuals with mutations in FMO3 present with accumulation of TMA levels, causing fish malodor syndrome (Treacy et al., 1998). TMAO appears to contribute to the development of atherosclerosis in part by promoting cholesterol accumulation within macrophages, perhaps by inducing scavenger receptors such as CD36 and SRA1, both of which are involved in the uptake of modified lipoproteins (Wang et al., 2011). One crucial question is how TMAO influences cellular metabolism and whether this is direct or indirect. Another important question relates to the nature of the variations in plasma TMAO levels in human populations and whether modulating TMAO levels can result in reduced risk of atherosclerosis.

We now report studies of the metabolism of TMA and TMAO in mice and humans. We examine the activities of the FMO family members and show that FMO3 is the most active in metabolizing TMA to TMAO. Using transgenic and adenoviral approaches, we show that up regulation of hepatic FMO3 decreases TMA and increases TMAO levels in the circulation, while antisense-mediated silencing of FMO3 increases TMA and decreases TMAO levels. We further show that FMO3 is dramatically down regulated by testosterone in mice, suggesting a mechanism for the greater susceptibility of female mice to atherosclerosis as compared to males, and that FMO3 expression is modestly decreased in males as compared to females in human populations. We also find that FMO3 is dramatically up-regulated by bile acids and that this is mediated by the action of the nuclear receptor FXR (NR1H4). Finally, we have examined natural variations of FMO3, TMAO, and atherosclerosis in mice. The results indicate that FMO3 contributes significantly to TMAO levels, that other factors must also be involved, and that TMAO explains about 11% of the variation in atherosclerosis susceptibility among common inbred strains of mice.

RESULTS

Expression levels and activities of flavin monooxygenase family members

Members of the FMO family are strong candidates for the conversion of TMA to TMAO (Treacy et al., 1998) and the five members of the family, FMOs 1 through 5, exhibit approximately 50% amino acid sequence identity, with high sequence conservation between mouse and human. We were interested in determining which of these related genes can metabolize TMA to TMAO. All five members of the family (human orthologues) were cloned into expression constructs, in either untagged form or tagged with the FLAG sequence at the N-terminus, and transfected into the human kidney cell line HEK293AD together with a plasmid expressing green fluorescent protein (GFP). As controls, cells were transfected with pcDNA (empty) or pcDNA expressing β -galactosidase. We did not detect any significant differences in transfection efficiency (as determined by GFP expression) (Fig. 1A; Suppl. Fig. 1A). Nonetheless, the relative over-expression of individual mRNAs corresponding to the individual FMO orthologues varied significantly (Fig. 1B, Suppl. Fig. 1B–E). Western blot assays utilizing antibody to the FLAG epitope demonstrated similar protein levels of FMO1, 3 and 5 in transfected cells, whereas the protein levels of FMO4 and FMO2 were relatively low (Fig. 1A). The low level of FLAG-tagged FMO2 protein relative to FMO1 and FMO3 was surprising as the mRNA levels for all three FMOs were

similar (Fig. 1B, Suppl. Fig. 1B, C), suggesting that FMO2 might be regulated by post-translational mechanisms.

We then determined the ability of the different FMOs (tagged and untagged) to metabolize TMA into TMAO by adding deuterated TMA (d9-TMA) to the transfected cells for 24 hours before collecting the media and measuring the levels of deuterated (d9)-TMAO by HPLC with on-line tandem mass spectrometry (see Methods) (Fig. 1C and D). Of the five FMOs, only FMO1 and FMO3 exhibited the ability to significantly oxidize TMA to TMAO, although very low levels of TMAO were detected in the media of cells transfected with the FMO2 plasmid (Fig. 1C). FMO3 was by far the most active FMO family member able to synthesize TMAO (Fig. 1C), and the activity was reflected by a reduction in the levels of the substrate TMA (Fig. 1D). Further, the 15-fold higher levels of TMAO production by FMO3 as compared to FMO1 (Fig. 1C) was observed despite similar cellular levels of both FLAG-tagged proteins (Fig. 1A). In addition, comparison of the enzymatic activities of FLAG-tagged with untagged constructs of FMO1 and FMO3 suggest that the FLAG epitope does not affect enzyme activity (Fig. 1C). Finally, Western blot assays using a specific antibody against FMO3 showed that tagged and untagged FMO3 protein levels were similar (Suppl. Fig. 1A). Based on these data, we determined the relative specific activities of FMO1 and FMO3 in transfected cells by dividing the levels of TMAO present in the medium by the cellular FMO protein (determined by densitometry of FLAG tagged protein). On this basis, the specific enzymatic activity of FMO3 is approximately 10-fold-higher than FMO1 (Fig. 1E). The very low activity and protein levels of FMO2 precluded accurate determination of a specific activity. These data, taken together, suggest that human FMO3 is likely the major enzyme capable of synthesizing TMAO from TMA. Consequently, we focus our efforts on the investigation of FMO3.

We first determined which tissues expressed FMO3, and among the various mouse tissues we examined, FMO3 mRNA levels were highest in the livers of female mice (Fig. 1F). As expected, FMO3 mRNA levels were lower (approximately 100-fold) in the livers of male mice (Fig. 1F). Adrenal FMO3 expression also exhibited a sexually dimorphic pattern (Fig. 1F). In contrast, male and female mice expressed similar levels of FMO3 in the aorta and lung (Fig. 1F). Thus, the sexual dimorphism that results in significant differences in tissue expression of FMO3 is limited to the liver and adrenals.

The data described above from overexpression studies indicate that the rank order of enzymatic activity is FMO3>FMO1>>FMO2. To determine the relative hepatic expression of these three genes *in vivo*, we analyzed RNA-Seq data obtained from male and female C57BL/6J mice. The data show that in females, hepatic FMO1 and FMO3 mRNA levels are expressed at similar levels, and FMO2 is expressed at lower levels (Fig. 1G). All three FMO mRNAs were expressed at lower levels in the livers of male mice compared to female mice (Fig. 1G).

We also determined whether the sexual dimorphic difference was maintained in human liver. We first analyzed expression data from 317 Caucasian human subjects and observed a significant difference in FMO1 and FMO3, but not FMO2, expression between males and females (Fig. 1H, Suppl. Fig. 1F) (Schadt et al., 2008). We also confirmed these differences by RT-qPCR in a random subset of subjects from the Genebank cohort (Bhattacharyya et al., 2008)(Fig. 1I).

Together, these results suggest that FMO3 in both humans and mice is the most active FMO family member able to synthesize TMAO from TMA, is highly expressed in liver, and exhibits sexual dimorphism. Based on these findings, we conclude that FMO3 contributes 90% of the total hepatic activity involving oxidation of TMA to TMAO.

FMO3 expression contributes to circulating TMAO levels

Having established that FMO3 can convert TMA to TMAO *in vitro*, we next sought to determine whether modulation of FMO3 levels *in vivo* would alter circulating plasma TMAO levels. Given that FMO3 is highly expressed in liver of female mice, but much lower in males, we carried out gain-of-function studies in males and loss-of-function experiments in female mice. First, we generated an adenovirus to overexpress mouse FMO3 in the liver. Seven days after adenovirus injection into male mice, FMO3 mRNA levels were overexpressed by 60-fold relative to basal levels in males (Fig. 2A), and this increase was accompanied by a large increase in FMO3 protein (Fig. 2B), which was only detectable in mice infected with the FMO3 adenovirus. Importantly, this was associated with a modest but significant increase in plasma TMAO levels (Fig. 2C). These results demonstrated that increased expression of FMO3 in the liver increases circulating plasma TMAO levels. However, we also noted that the fold increase in FMO3 mRNA and protein was far greater than the corresponding change in plasma TMAO, suggesting that additional mechanisms are involved in the regulation of plasma TMAO levels. To determine the effect of persistent hepatic overexpression of FMO3 *in vivo*, we generated FMO3 transgenic mice by overexpressing human FMO3 from a liver-specific albumin promoter (see Supplemental Methods). Three founders carrying the transgene were identified and all exhibited moderate overexpression of both FMO3 mRNA and protein (data not shown). We selected males from the line with the highest FMO3 expression for further study (Suppl. Fig. 2A–B). The transgenic mice and wild-type littermate controls were given drinking water supplemented with choline (1.3%), the precursor of TMA. After 7 days the plasma TMAO levels were significantly higher in FMO3 transgenic mice as compared to littermate controls (Suppl. Fig. 2C). Similar effects were observed in the other FMO3 transgenic lines (data not shown).

To examine the effects of reduced FMO3 expression, we utilized a specific FMO3 antisense oligonucleotide (ASO). Treatment of female mice with the ASO resulted in more than 90% reduction in liver FMO3 mRNA levels (Fig. 2D) as well as a 50% decrease in FMO3 protein levels (Fig. 2E). This resulted in a 47% decrease in plasma TMAO levels (Fig. 2F) and over 2-fold increase in plasma TMA levels in FMO3 ASO-treated mice relative to vehicle-treated controls (Suppl. Fig. 2D). ASO treatment did not result in abnormal plasma ALT and AST levels, indicating normal liver function, although there was a small but statistically significant increase in ALT levels in ASO treated mice (Suppl. Fig. 2E).

Based on these results, we conclude that FMO3 is the rate-limiting enzyme in the conversion of TMA to TMAO. Increased hepatic expression of FMO3 protein *in vivo* results in decreased TMA and increased plasma TMAO, whereas decreased expression of FMO3 has the reciprocal effect. It is also clear that the change in FMO3 mRNA and protein are not necessarily reflected in TMAO levels, indicating that post-transcriptional events and/or alternative mechanisms are likely involved in regulating plasma TMAO levels.

Dietary and sex-biased regulation of FMO3 and TMAO

As shown above (Fig. 1F–G), mice exhibit dramatic sex-specific differences in hepatic FMO3 expression. To investigate this further, we examined the effects of choline-enriched diet on hepatic FMO3 gene expression, expression and enzymatic activity, as well as plasma TMA and TMAO levels in male and female mice (Fig. 3). Supplementation of the control diet with choline (1%), which greatly increases TMA production by the gut flora (Zeisel et al., 1989) did not affect the expression of hepatic FMO3 in either female or male mice (Fig. 3A). However, compared to a chow diet, choline supplementation in both males and females resulted in a very large increase in plasma TMAO levels (Fig. 3B). The increase in plasma TMAO levels was more pronounced in females than in males (Fig. 3B), consistent with higher hepatic FMO3 expression in female mice. Conversely, the levels of the precursor

metabolite TMA were much higher in male than female mice fed the choline-enriched diet (Fig. 3C). The observation that males had higher levels of TMA is consistent with a reduced capacity to synthesize TMAO in the presence of presumably a large excess of the substrate TMA derived from dietary choline. These changes were not due to altered FMO activity as the ability of liver homogenates to oxidize TMA to TMAO was independent of the diet (Fig. 3D), although there were the expected differences between males and females.

Gender differences in plasma TMAO levels could also be caused by altered fractional excretion of TMAO. In female mice, we found no significant differences in fractional excretion rates of TMAO between mice fed either a choline-rich or control diet in females (Suppl. Fig. 3A). In contrast, males had a small but statistically significant increased fractional excretion rate compared to females fed the same control diet, (Suppl. Fig. 3A), but these results are unlikely to explain the observed differences in TMAO levels. To investigate possible differences in gut flora between genders, we isolated microflora from different regions of the intestine from male and female mice and measured their ability to convert cholintrimethyl-d₉ (d₉-choline) to trimethylamine-d₉ (d₉-TMA). The levels of activity were higher in the cecum compared to the jejunum, but no significant differences were observed between males and females (Suppl. Fig. 3B). Together, these results suggest that the differences in circulating TMAO levels in male and female mice are not due to differences in aerobic intestinal bacterial flora.

To determine if the gender effects present in mice were also observed in humans, we examined plasma TMAO levels in random samples from patients from the Genebank cohort. Surprisingly, we were unable to detect any difference in circulating TMAO levels (Suppl. Fig. 3C). Similar to our studies in mice we did not observe any difference in the fractional excretion rate of TMAO in a separate cohort of 20 male and female subjects (Suppl. Fig. 3D).

These collective observations, although consistent with a rate-limiting effect of FMO3 on the conversion of TMA to TMAO, suggest that dietary components can have a major effect on the synthesis of TMAO. This may be particularly relevant for diets rich in choline-containing products. Thus, any sex-related differences in plasma TMAO levels may have been obscured as a result of varied diets across the human population.

Hormonal regulation underlying sexual dimorphism of FMO3 expression and TMAO levels

To investigate the mechanism underlying the observed gender differences, we examined the effects of testicular and ovarian hormones on hepatic *Fmo3* gene expression. First, we utilized either intact or gonadectomized (GDX) C57BL/6J males either treated with dihydrotestosterone (DHT) or placebo. Conversely, we also compared intact and ovariectomized (OVX) C57BL/6 female mice treated with either estradiol (E2) or placebo (Fig. 4). Compared to intact male mice, GDX-males exhibited over a 100-fold increase in hepatic *Fmo3* mRNA levels, as well as increased FMO3 protein and a 7-fold increase in plasma TMAO (Fig. 4A–C). Treatment of the GDX-males with DHT caused a profound decrease (90%) in FMO3 mRNA, protein and plasma TMAO (Fig. 4A–C). Together, these data suggest that the low hepatic expression of FMO3 is at least partly a result of repression by androgens/dihydrotestosterone. In females, ovariectomy caused a modest decrease in hepatic FMO3 expression, protein and plasma TMAO levels (Fig. 4A–C). Interestingly, treatment of OVX-females with estrogen resulted in a small but significant increase in hepatic FMO3 mRNA and protein and in plasma TMAO levels (Fig. 4A–C).

In addition to acute hormonal effects, sex differences can also result from differences in development and the sex chromosomes. We assessed such potential by profiling livers from the “four core genotype” mice, consisting of XX females, XX males, XY females, and XY

males. These were generated using deletion (XY females) or transgenic expression (XX males) of the testes factor determining gene (Arnold and Burgoyne, 2004). To eliminate the acute effects of sex hormones, the mice were gonadectomized at 10 weeks of age. We could not detect any differences in FMO3 gene expression among the FCG strains (Suppl. Fig. 4), indicating that the effects of gender on FMO3 expression are due entirely to hormonal effects rather than permanent alterations to FMO3 during development.

Taken together, these results indicate that testosterone is largely responsible for the reduced hepatic FMO3 expression observed in males, and the estrogen-dependent induction of FMO3 expression may further exacerbate the gender differences. The concordant increase in hepatic FMO3 and plasma TMAO in GDX-males is consistent with the rate-limiting role of FMO3 in TMA oxidation.

Regulation of FMO3 by FXR

In preliminary studies of mice carrying a transgene for the human ApoB100 gene (hApoB100), we noted that a high-fat, cholesterol-containing diet (HF) supplemented with the bile acid, cholic acid, (HF+CA) resulted in increased atherosclerosis and hepatic FMO3 expression, as compared to mice fed the HF diet. To investigate whether the increase in FMO3 levels was specifically due to the presence of dietary cholic acid, we fed five inbred strains that carry the hApoB100 transgene either the HF or HF+C diet and determined FMO3 expression and plasma TMAO levels. As shown in Figure 5A–D, hepatic FMO3 mRNA and circulating plasma TMAO levels were increased in the presence of dietary cholic acid, suggesting bile acids regulate FMO3 activity in both male and female mice.

Many effects of bile acids on gene expression are mediated via activation of the nuclear hormone receptor Farnesoid X Receptor (FXR, *Nr1h4*). To investigate whether FXR could regulate *Fmo3* gene expression and TMAO levels *in vivo*, we utilized a combination of loss- and gain-of function approaches. Given that hepatic FMO3 expression was profoundly different in males and females, we decided to treat both male and female wild-type (C57BL/6) or *Fxr*^{-/-} mice for 3 days with either vehicle or GSK2324, an FXR-specific agonist (Bass et al., 2011). As a positive control we showed that GSK2324 treatment of both male and female wild-type, but not *Fxr*^{-/-} mice, led to induction of the well characterized FXR target gene *Bsep/ABCB11* (Fig. 6A). As expected, the basal expression levels of *Bsep* and the fold induction after FXR activation were similar for both male and female mice (Fig. 6A). Induction of hepatic FMO3 by GSK2324 was also only observed in wild type but not *Fxr*^{-/-} treated mice (Fig. 6B). However, in contrast to *Bsep*, the fold induction of FMO3 in the livers of wild type males was far greater than was observed in female mice (~20-fold versus ~2.5-fold increase) (Fig. 6B). Nonetheless, FXR activation with GSK2324 led to increased plasma TMAO levels in wild-type male and female mice, but not *Fxr*^{-/-} mice (Fig. 6C). These findings suggest that FMO3 might be a direct target of activated FXR, resulting in increased conversion of TMA to TMAO. The finding that basal FMO3 mRNA levels were similar in wild type and *Fxr*^{-/-} mice of the same gender (Fig. 6B) suggests that basal FMO3 mRNA levels are independent of FXR, but dependent upon gender.

To further characterize the induction of FMO3, we next utilized an alternative FXR agonist (GW4064) together with wild type mice or mice that lack FXR in the liver (L-KO) or intestine (I-KO). The studies demonstrated that GW4064 induced hepatic FMO3 at least 17-fold in wild type and I-KO mice, but failed to induce FMO3 mRNA levels in L-KO mice (Suppl. Fig. 5A–C). Consequently, we conclude that induction of hepatic FMO3 is dependent upon hepatic but not intestinal FXR. In addition, FXR activation modestly induced hepatic FMO2 (2-fold) without affecting FMO1 or FMO4 mRNA levels (Suppl. Figure 5D–F). This suggests some degree of coordinate regulation of FMO3 and FMO2 which physically reside at the same chromosome locus (Suppl. Fig. 6D–F). Taken together,

these results demonstrate coordinate regulation of FMO3 and plasma TMAO levels by the FXR agonists GSK2324, GW4064 and cholic acid.

To identify the molecular mechanism involved in the induction of FMO3 by FXR, we next utilized two independent ChIP-Seq genome wide surveys of FXR binding sites (Chong et al., 2010; Thomas et al., 2010). We identified three FXR Response Elements (FXREs) near the *Fmo3* gene locus, including one in the proximal promoter region 1.8kb upstream of the transcriptional start site (* in Sup. Fig. 6). To determine whether the FXRE in the proximal promoter was functional, we generated an *Fmo3* promoter-luciferase reporter plasmid and transfected it into Hep3B cells, a human hepatoma cell line. FXR overexpression and activation with the GSK2324 caused a dose-dependent increase in FMO3 promoter-driven luciferase reporter activity (Fig. 6D). The FXR-dependent effect was completely abolished when the FXRE in the *Fmo3* promoter was mutated (Fig. 6D), indicating that FMO3 is a direct FXR target gene.

We also investigated possible regulation of FXR target genes by the TMA-FMO3-TMAO pathway. Preliminary data obtained after feeding male *apoE*^{-/-} mice normal chow or chow supplemented with either choline (1%) or TMAO (0.12%) suggests that these diets do not significantly affect the expression of the FXR target genes *Shp* and *Bsep* (data not shown).

Natural variation affecting FMO3 regulation, TMAO levels, and atherosclerosis

We surveyed two panels of inbred strains of mice to identify common genetic factors contributing to FMO3 expression or plasma TMAO levels. To identify genetic variants regulating FMO3 levels we queried a database containing expression data for the Hybrid Mouse Diversity Panel (HMDP, <http://systems.genetics.ucla.edu/>). This panel consists of about 100 inbred strains of mice that have been fully genotyped and characterized for various clinical intermediate phenotypes such as gene expression. This panel has unprecedented mapping resolution and has sufficient power to map genes contributing to 5% or more of the overall trait variance (Bennett et al., 2010; Ghazalpour et al., 2012). FMO3 expression varied significantly among the HMDP strains and the major locus regulating expression mapped directly over the FMO3 gene, at 164 Mb on Chromosome 1, suggesting *cis*-acting regulation (Fig. 7A, red dots). This variation of FMO3 allowed us to examine the relationship between FMO3 expression, TMAO levels, and atherosclerosis. We therefore surveyed an additional panel of 22 strains of mice carrying a hyperlipidemia-inducing human apolipoprotein B gene (Bennett et al., 2012). There was a clear relationship between the variation of FMO3 expression and the levels of plasma TMAO when both males and females were examined ($r=0.57$, $p<0.001$) (Fig. 7B). The strains were previously typed for atherosclerosis susceptibility, with males exhibiting much smaller lesions than females (Bennett et al., 2012). We measured plasma TMAO levels in mice of each strain ($n=3-8$ mice/strain) (Fig. 7C) and observed a significant correlation between TMAO and atherosclerosis in females ($r=0.34$, $p<5\times 10^{-5}$) (Fig. 7D). Most of the males exhibited few significant lesions and the correlation with TMAO was not significant (data not shown). We did not observe any differences in lesion morphology that correlated with TMAO levels (data not shown). Based on the results with female mice, we conclude that TMAO explains about 11% (r^2) of the total variation of atherosclerosis among common inbred strains included in the panel.

Our studies have demonstrated that FMO3 expression is genetically regulated and that FXR is a crucial regulator of FMO3 levels. Thus, we next investigated if there are natural variations localized near any of the FXREs identified by ChIP-Seq analysis (Suppl. Fig. 6) and if these variations lead to differences in FXR mediated FMO3 transcription. We first cloned the 2.5kb promoter region of FMO3 from 8 strains of mice into a luciferase reporter plasmid and determined that FXR activation of FMO3 was not affected by the genetic variation in

the promoter region (Suppl. Fig 7). Our analysis identified one SNP that was adjacent to an intronic FXRE that was associated with variation of FMO3 expression at genome-wide significance levels (arrow in Fig. 7E). We then made luciferase reporter plasmids containing 3 copies of the FXRE and flanking region containing either SNP (A or G). FXR activation of the reporter plasmid was significantly affected, with the FXRE containing the G SNP having a much lower activity (Fig. 7F). Taken together, these results indicate that genetic variation of FMO3 expression is at least partly mediated by the nuclear receptor FXR.

DISCUSSION

Wang and colleagues (Wang et al., 2011) recently reported a striking relationship between the levels of TMAO and atherosclerosis in a large population of heart disease patients and controls, and studies in mice were consistent with a causal relationship. Understanding the factors that regulate circulating levels of TMAO is therefore clearly important if pharmacologic strategies are to be employed to modulate TMAO levels. FMO3 was considered a strong candidate for the conversion of TMA to TMAO, since a human disorder characterized by elevated TMA levels and resulting in a pungent odor, termed fish malodor syndrome, had been shown to be the result of FMO3 mutations (Treacy et al., 1998). We have now further investigated factors contributing to TMAO metabolism in both humans and mice. A number of conclusions have emerged. First, three members of the FMO family are shown to be capable of oxidizing TMA to TMAO, although FMO3 exhibits the highest specific activity. Second, using over-expression and antisense-mediated silencing in mice, FMO3 expression is shown to significantly affect both TMA and TMAO levels. Third, FMO3 expression and TMAO levels in mice are shown to exhibit a strong gender bias, and testosterone inhibition of FMO3 expression is shown to underlie the gender difference. Fifth, levels of TMAO and FMO3 expression are regulated by the nuclear receptor FXR. Finally, studies of natural genetic variations in mice are consistent with a role of FMO3 in controlling TMAO levels and a role of TMAO levels in atherosclerosis susceptibility. Each of these points is discussed in turn below.

The FMO family (reviewed in (Cashman and Zhang, 2006) consists of five family members, FMO1-5, and we expressed each human FMO in tissue culture cells and measured the ability of lysates to convert TMA to TMAO. These studies indicated that several members, FMO1, FMO2, and FMO3, exhibited some level of activity. Using FLAG-tagged FMO expression plasmids, we show that FMO3 exhibited about 10-fold greater specific activity than FMO1. The specific role of FMO2 in regulating TMAO levels is confounded by the reduced protein levels. Based on hepatic expression levels in mice and humans, we concluded that FMO3 accounted for the majority of the activity, with the exception of male mice, which exhibited very low levels of FMO3. Since FMO1 expression is very high in the male liver, and FMO1 has the ability to convert TMA to TMAO, we speculate that FMO1 may be partly responsible for TMAO synthesis in male mice. While the liver was the major site of expression of the FMOs, it is noteworthy that the adrenals, lung and aorta also expressed substantial FMO3, raising the possibility of extra-hepatic conversion of TMA to TMAO.

In vivo loss- and gain-of-function experiments demonstrated that FMO3 expression is a major regulator of TMAO levels. However, fold changes in hepatic FMO3 mRNA or protein levels are generally far greater than the corresponding changes in circulating TMAO levels. This is particularly true in male mice. This discrepancy is consistent with other factors contributing to TMAO synthesis. This may include FMO1 and possibly FMO2, or post-transcriptional modifications of FMO3 that enhances activity. This warrants further investigation and may represent a pathway that can be targeted pharmacologically. Since loss of FMO3 expression causes fish malodor syndrome, it would not be a straight forward

pathway to target in order to reduce TMAO levels. However, if activity can be modulated, perhaps the undesirable effect of TMA accumulation can be diminished or avoided.

We also investigated the molecular mechanisms for the effects of both gender and bile acids on the expression of FMO3 and TMAO levels. In mice, females had much greater hepatic expression and protein levels of FMO3 as compared to males, and the difference was approximately 100-fold in most strains of mice. Whereas females exhibited higher levels of plasma TMAO than males, the reverse was true of TMA levels, indicating that female mice exhibit more efficient conversion of TMA to TMAO. Since hepatic FMO3 levels are also elevated in females, and correlate significantly with plasma TMAO levels, it appears that FMO3 is the primary cause for differences in TMAO levels between male and female mice. In humans, males also exhibited reduced levels of FMO3 expression as compared to females, although the differences were much more modest. However, in contrast to mice, there were no discernible differences in circulating TMAO levels between genders in a human population. We attribute these differences to the varied diet consumed by humans. Given that FMO3 and TMAO levels are largely affected by diet, any differences in TMAO between sexes would likely be obscured. In addition, our studies with GXD- or OVX-treated mice indicate that differences in FMO3 expression and TMAO levels also appear to be under strong hormonal control. This notion is supported by human studies where it has been reported that menstruation can induce transient trimethylaminuria (high levels of TMA in urine) (Shimizu et al., 2007) and that plasma TMAO levels are reduced in menopausal women (Spencer et al., 2012). This latter observation is consistent with our findings in mice that estrogen promotes hepatic FMO3 expression. The reason for these striking differences in mice, as compared to the modest differences in humans, is unknown, but may relate to the processing of pheromones that affect sexual behaviors. Pheromones are important cues in mating in mice [reviewed in (Touhara and Vosshall, 2009)] and FMO3 could affect the oxidation of some of these pheromones. Alternatively, TMA or TMAO could have pheromone-like effects. Conceivably, the elevated levels of TMA during menstruation could act as a sexual deterrent.

We have examined the effects of various diets on TMAO metabolism in mice, and observed that diets containing cholic acid, induced hepatic FMO3 mRNA and protein as well as plasma TMAO levels. Dietary supplementation with cholic acid has long been known to promote atherosclerosis (Paigen et al., 1987). Our current studies suggest for the first time that this increase in atherosclerosis may be due in part to the activation of FXR and the subsequent elevation of FMO3 and synthesis of TMAO, in addition to the effect of bile acids on lipoprotein levels. These conclusions are based on the observations that cholic acid induction of FMO3 was mediated by the bile acid-activated nuclear receptor FXR, that FMO3 is a *bona fide* FXR target gene, and that activation of FXR *in vivo* is accompanied by an increase in plasma TMAO levels.

FXR has previously been shown to regulate several phase II and phase III xenobiotic genes (Lee et al., 2010) and the various FMO genes are also thought to function as phase I xenobiotic genes (Lefebvre et al., 2009). The regulation of FMO3 by FXR provides a potential target for therapeutic modulation of TMAO levels, although the broad metabolic effects of FXR, including the relationship with hepatic lipoprotein and bile acid metabolism, may restrict such therapeutic applications. FXR activation has been shown to protect mice from atherosclerosis (Hartman et al., 2009). Nonetheless, the induced FMO3 and TMAO levels would raise some concerns about the use of FXR agonists as therapeutic agents. Our data also reveal a mechanism for the complex relationship between FXR and atherosclerosis, and the disparate atherosclerosis results observed in several FXR knockout studies (Hageman et al., 2010; Zhang et al., 2006). Given that the precise functions of TMAO

remain to be identified, it will be important to determine what role TMAO plays following FXR activation.

Our studies have focused on total transcript and protein levels of FMO genes, but additional mechanisms of regulation, such as alternative splicing and post-transcriptional regulation could account for differences between transcriptional activation and FMO activity. Previous reports (Lattard et al., 2004) and recent data from the 1000 genomes project (Altshuler D, 2010) have identified multiple splice variants for the human FMO1, FMO2 and FMO3 genes. In the case of FMO3 there are 9 splice variants of which 4 are protein coding and 5 are processed transcripts. At least 2 of these splice variants affect the catalytic activity of human FMO1 and FMO3 (Lattard et al., 2004) and may indicate an important factor affecting TMAO production. In addition to isoform variation, there is some evidence that nitric oxide reduces FMO1 mRNA stability and FMO3 activity through a post-transcriptional modification (Ryu et al., 2004a; Ryu et al., 2004b). Further study is necessary to determine the functional impact of individual FMO isoforms and possible post-transcriptional modifications on TMA oxidation and ultimately, cardiovascular risk.

A long-term goal of our work is to understand the natural variations of TMAO metabolism in human populations. We have performed limited genome-wide association studies of human populations and, thus far, these have not been informative in terms of identifying loci controlling TMAO levels (unpublished results). This may be related to the large perturbations in TMAO levels resulting from dietary differences. It may also be attributable to the fact that intestinal microflora more so than a somatic genetic factor, play a more prominent role in variation of TMAO levels. Although the specific genetic variations contributing to TMAO levels in human populations are unlikely to be the same as those that occur in mouse populations, the pathways are likely to be shared, at least in part. Therefore, we investigated FMO3, TMAO, and atherosclerosis among two panels of mouse strains, one on a hyperlipidemic genetic background. We found that there was considerable variation in FMO3 expression among strains and that the FMO3 variations influenced TMAO levels, consistent with our targeted studies. Overall, TMAO levels explained about 11% of the differences in atherosclerosis susceptibility in females in the 22 strains investigated, roughly consistent with human population studies (Wang et al., 2011). Preliminary studies by Wang et al. (Wang et al., 2011) suggested that TMAO levels increase the formation of cholesterol-engorged macrophages and that this might occur through up-regulation of scavenger receptors for modified lipoproteins. Our results, particularly those indicating a role of bile acids in TMAO levels, further hint that the mechanism(s) by which TMAO affects atherosclerosis may involve lipids. Our studies in mice also clearly indicate that FMO3 only partly explains the variations in plasma TMAO levels. Other likely factors include other enzymes that can metabolize TMA to TMAO, including FMO1, or perhaps FMO2, and most prominently, gut flora composition. Numerous reports in the literature have shown that there is genetic control of the composition of gut flora (Benson et al., 2010; Dumas et al., 2006; Kovacs et al., 2011; Turnbaugh et al., 2010). However, to date we are unaware of any direct evidence linking alterations in one microbial population affecting TMAO levels in humans or mice. Gender differences in TMAO levels in mice were not due to differences in the production of TMAO in cultures of gut flora between sexes of mice. These studies were specific to aerobic species and we cannot rule out that there were differences from anaerobic bacteria.

In conclusion, our study extends our previous findings (Wang et al., 2011) and supports a causal relationship between FMO3 expression, TMAO levels, and atherosclerosis. Clearly, the relationship is affected by gender (at least in mice) and dietary factors. The identification of regulatory factor(s) affecting TMAO levels provides possible target(s) for therapeutic intervention in fish malodor syndrome and atherosclerosis.

EXPERIMENTAL PROCEDURES

Mice, Diets, and Treatments

C57BL/6J mice were purchased from The Jackson Laboratory (Bar Harbor, ME). All mice were maintained on a 12-hour light dark cycle and fed a standard chow diet (NIH31 modified mouse/rat diet, catalogue no. 7013, Harlan Teklad) *ad libitum*. For gonadectomy/ovariectomy experiments, C57BL/6J were gonadectomized at 8 weeks of age, implanted with hormone pellets at 12 weeks, and killed at 14 weeks. Male and female mice of the hormone-treated groups received subcutaneous implants of either 0.5 mg estradiol pellet or a 5mg dihydrotestosterone pellet to release over 21 days. Control mice were treated with the placebo pellet (Innovative Research of America; placebo, catalog item no. C-111). For FMO3 ASO studies, four 6–8 weeks old female C57BL/6 mice per group, on chow diet, received 7 once weekly intraperitoneal injections of saline or the Fmo3 ASO at a dose of 50 mg/kg body weight. Mice were euthanized and plasma and liver tissue collected. For atherosclerosis studies, ApoB-100 Tg mice were purchased from Taconic and bred with 13 inbred strains purchased from the Jackson labs as previously described (Bennett et al., 2012). The mice were fed Purina Chow containing 4% fat until 8 weeks of age, and then transferred to a high-fat diet (37% fat) containing cholesterol (1.25%) and cholic acid (0.5%), Harland Teklad TD.88051. A subset of mice were placed on high-fat, cholesterol-containing diet but without cholic acid (Teklad Western TD.88137). For FXR studies, male or female 10–12-week-old mice wild-type and *Fxr*^{-/-} mice (backcrossed to C57BL/6J mice for 10 generations at UCLA) were treated with either vehicle (water) or GSK2324 (Bass et al., 2011) at 30 mpk, once a day for 3 days. All animal experiments were approved by the Office of Animal Research Oversight (OARO) at UCLA.

Quantification of TMAO, TMA and Creatinine

Quantification of TMAO and TMA in mouse plasma was performed using stable isotope dilution HPLC with on line electrospray ionization tandem mass spectrometry on an API 365 triple quadrupole mass spectrometer (Applied Biosystems, Foster, CA) with upgraded source (Ionics, Bolton, ON, Canada) interfaced with a Cohesive HPLC (Franklin, MA) equipped with phenyl column (4.6 × 2505mm, 5 μm Rexchrom Phenyl; Regis, Morton Grove, IL) and the separation was performed as reported previously (Wang et al., 2011). TMAO and TMA were monitored in positive MRM MS mode using characteristic precursor–product ion transitions: m/z 76 58, m/z 60 44 and m/z 114 86, respectively. The internal standards TMAO-trimethyl-d9 (d9-TMAO) and TMA-d9 (d9-TMA) were added to plasma samples before sample processing, and were similarly monitored in MRM mode at m/z 85 68, m/z 69 49 and m/z 117 89. Various concentrations of TMAO and TMA standards and a fixed amount of internal standards were spiked into control plasma to prepare the calibration curves for quantification of plasma TMAO and TMA. For d9-TMA and d9-TMAO quantification in FMO activity analyses, 1,1,2,2-d4 choline (Sigma) was used as an internal standard followed by a 0.5 ml 3K cut-off centrifugal filter (Millipore) of sample prior to LC/MS/MS analysis. The characteristic precursor–product ion transition for 1,1,2,2-d4 choline is m/z 108 60 monitored in positive MRM MS mode.

FMO3 Antisense Oligonucleotide (ASO)

A chimeric 20-mer phosphorothioate oligonucleotide targeted to mouse *Fmo3* (5'-TGGAAGCATTTGCCTTTAAA-3') containing 2 -O methoxyethyl (MOE) groups at positions 1–5 and 15–20 was synthesized and purified as described (Baker et al., 1997) with an automated DNA synthesizer (380B, Perkin-Elmer-Applied Biosystems, Foster City, CA). Plasma TMAO and TMA levels were determined using LC/MS. Liver RNA was isolated and examined for the expression of FMO3 mRNA by the Taqman probe based gene expression analysis and liver was also homogenized to determine FMOs activity.

Human Studies

Plasma TMAO levels were determined from sequential consenting subjects seen in the cardiology clinic, at the Cleveland Clinic and enrolled in the GeneBank study. Details about this cohort have been previously described (Bhattacharyya et al., 2008; Wang et al., 2011). Liver tissue from humans came from residual liver biopsy material collected at the time of diagnostic evaluation during surgery. All subjects gave informed consent and all studies were approved by the Cleveland Clinic Institutional Review Board. Microarray data from human liver samples were downloaded from GEO ([GSE9588](#)), inverse log10 transformed and expressed as a fold difference between males and females.

FMO1-5 Plasmid Construction

Human FMO1-5 cDNAs were cloned from cDNA generated from total RNA derived from Hep3B or HepG2 cell lines (ATCC). Each cDNA sequence was amplified by PCR using specific primers containing a Kozak site upstream of the ATG and cloned into pcDNA3.1 plasmid (Life Technologies). For FLAG-tagged plasmid construction, cDNA sequences for FMO1-5 were re-amplified using the primers containing Gateway att sequences (Life Technologies), without the ATG start codon, and cloned into pDONR221 plasmid (Life Technologies). DONR plasmids were recombined into a Gateway-adapted pcDNA3.1 plasmid containing an N-terminal FLAG sequence using LR clonase (Life Technologies) according to manufacturers instructions.

Cell Culture

HEK293Ad cells (Agilent) or Hep3B (ATCC) cell lines were cultured according to ATCC recommendations. For FMO1-5 activity assays, HEK293Ad cells were seeded in 6- or 12-well plates at 70–80% confluence. Cells were transfected with 900ng/well (6-well) or 450ng/well of pcDNA FMO1-5, pcDNA N-FLAG FMO1-5, pcDNA3.1 and pcDNA3.1 LacZ plasmids. To determine transfection efficiency, cells were co-transfected with pSicoR GFP plasmid (100ng/well for 6-well or 50ng/well for 12-well plates). Transfection was carried out after cells were washed and placed in OPTI-MEM, using FugenHD (Promega) as the transfection reagent according to manufacturers instructions. For Fmo3 promoter studies, the 3kb region upstream of the mouse *Fmo3* gene was cloned into pGL4.10 plasmid (Promega). Hep3B cells were seeded 24h prior to transfection in 48-well dishes. The following day, cells were transfected with FMO3 reporter constructs and increasing concentrations of pcDNA3.1 FXR 2 expression plasmid for 24h in OPTI-MEM using Fugene HD (Roche). Transfection medium was removed and cells were treated with either vehicle (water) or GSK2324 (1 μ M) in medium containing 10% charcoal-inactivated serum (Omega) for a further 24h before being harvested. Luciferase activity was determined using Luciferase Assay System (Promega) and normalized to β -gal activity to correct for variations in transfection.

Determination of Enzymatic Activity of Flavin Monooxygenases (FMOs)

For cell culture studies, HEK293Ad cells transfected with FMO1-5 were treated 24 h post-transfection with 100 μ M d9-TMA and media was collected and snap frozen in liquid nitrogen. Deuterated TMAO and TMA levels were determined as described above. Determination of enzymatic activity of hepatic FMOs was conducted in 250 μ l reaction mix containing 1 mg liver protein homogenate, 100 μ M d9-TMA and 100 μ M reduced nicotinamide adeninedinucleotide phosphate (NADPH) in 10 mM Hepes, pH 7.4. Reaction was stopped 8 hours later with 0.2 N formic acid, followed by filtering through a 3 K cut-off spin filter, and then snap frozen and stored at -80°C until time of analysis. For analyses, internal standard was added to the thawed filtrate, which was then injected onto an HPLC column with on-line tandem mass spectrometer to measure the oxidized product d9-TMAO

as described above. Control studies performed omitting NADPH did not show conversion of TMA into TMAO.

Adenovirus Preparation

Mouse *Fmo3* cDNA was amplified from cDNA synthesized from female liver C57BL/6 total RNA and cloned into pAdTrack CMV plasmid. Control adenovirus was made from an empty pAdTrack CMV plasmid. AdTrack, or AdTrack *Fmo3* were recombined into pAdeasy plasmid in BJ5183 cells (Agilent) and adenovirus particles were prepared using the AdEasy system (Agilent). High-titer adenovirus particles were purified by CsCl gradient centrifugation and dialyzed for 48 hours and stored at -80°C . Particles were quantified by serial dilution methods and detection of GFP positive plaques in HEK293Ad cells (Agilent). For *in vivo* overexpression, 10^9 plaque forming units (PFU) were injected into the tail vein of 10–12 week old male C57BL/6 mice. Livers and plasma were collected 7 days post-infection after a 4–5 hour fast.

Real Time PCR

Total RNA was isolated in QIAzol using the RNeasy kit (QIAGEN) according to the manufacturer's instructions. Gene expression was determined from cDNA synthesized using Reagents for Taqman kit (Applied Biosystems) from 500 ng of total RNA and using a Lightcycler 480 Real-time qPCR machine and Lightcycler 480 Mastermix (KapaBiosystems). Relative gene expression was determined using an efficiency corrected method and efficiency was determined from a 3-log serial dilutions standard curve made from cDNA pooled from all samples. Primers were designed across exon-exon boundaries using Roche UPL guidelines. Results were normalized to *Tbp*, *36B4* or *-actin* mRNA.

RNA-Seq Experiments

Liver polyA mRNA was isolated from (DBA2J \times C57BL) F1 mice, and libraries were prepared as recommended by the manufacturer (Illumina, Hayward, CA, USA). The samples were sequenced using the Illumina GAIIIX sequencer to a coverage of approximately 40 millions single end reads of 75 bp. These were aligned to the mouse reference genome mm9 allowing for up to 5 mismatches as described (Trapnell et al., 2009)

Western Blot Analyses

Whole liver lysates were homogenized, or cell lysates were scrapped in RIPA buffer (1 \times PBS with 1% SDS, 5g/L Sodium deoxycholate, 1% NP-40) supplemented with protease inhibitor cocktail (Roche) fortified with additional PMSF, Leupeptin, Aprotinin and ALLN (Sigma) and quantified using the BCA assay (Pierce). Equal amounts of protein (30 μg for male mice, and 10 μg for female mice) were separated on 4–12% acrylamide gels (BioRad) and transferred to a PVDF membrane (Millipore). Membranes were blocked for 16 hours in 5% non-fat milk solution in Tris-Buffered Saline containing 0.5% Tween 20 and probed with antibodies to FMO3 (ABCAM, Ab126790), mouse monoclonal β -Actin (Sigma), GAPDH (Genetex) or FLAG (Sigma Cat# F1804) for 1–3 hours. HRP detection was carried out using ECL plus reagent (GE Healthcare) according to manufacturer's instructions. Densitometric analysis was carried out using Quantity One software (BioRad).

Statistical Analysis

Statistical analysis was performed using Prism Graphpad software (V5.0) or Microsoft Excel. Comparison between control and treatment group(s) was carried out using either a student t-test or One-way ANOVA and statistical significance is shown as described in the figure legends.

Supplementary Material

Refer to Web version on PubMed Central for supplementary material.

Acknowledgments

The authors thank Drs. Timothy Willson and David Deaton (GSK) for the kind gift of GSK2324 as well as Nam Che, Kristy Ou, and Tammy Kim for excellent technical assistance.

Grant Support: This research was supported in part by PO1 HL30568 NIH/NHLBI and PO1 HL28481 NIH/NHLBI (AJL), R01HL103866 and P20HL113452 (SLH), K99/R00 HL102223 (BJB), P01 HL30568 (PAE), an AHA Scientist Development Grant 12SDG12050473 (ZW), the Howard Hughes Med Into Grad Scholar program and the Molecular Medicine training grant from NIH National Institute of General Medical Sciences T32GM088088 (JG) and AHA post doctoral fellowship 11POST7240070 (T Q de AV). SLH was also partially supported by a gift from the Leonard Krieger Fund.

REFERENCES

- Altshuler D, D R, Abecasis GR, Bentley DR, Chakravarti A, Clark AG, Collins FS, De La Vega FM, Donnelly P, Egholm M, Flicek P, Gabriel SB, Gibbs RA, Knoppers BM, Lander ES, Leibrach H, Mardis ER, McVean GA, Nickerson DA, Peltonen L, Schafer AJ, Sherry ST, Wang J, Wilson R, Gibbs RA, Deiros D. A map of human genome variation from population-scale sequencing. *Nature*. 2010; 467:1061–1073. [PubMed: 20981092]
- Arnold AP, Burgoyne PS. Are XX and XY brain cells intrinsically different? *Trends Endocrinol Metab*. 2004; 15:6–11. [PubMed: 14693420]
- Baker BF, Lot SS, Condon TP, Cheng-Flournoy S, Lesnik EA, Sasmor HM, Bennett CF. 2'-O-(2-Methoxy)ethyl-modified anti-intercellular adhesion molecule 1 (ICAM-1) oligonucleotides selectively increase the ICAM-1 mRNA level and inhibit formation of the ICAM-1 translation initiation complex in human umbilical vein endothelial cells. *J Biol Chem*. 1997; 272:11994–12000. [PubMed: 9115264]
- Bass JY, Caravella JA, Chen L, Creech KL, Deaton DN, Madauss KP, Marr HB, McFadyen RB, Miller AB, Mills WY, Navas F 3rd, Parks DJ, Smalley TL Jr, Spearing PK, Todd D, Williams SP, Wisely GB. Conformationally constrained farnesoid X receptor (FXR) agonists: heteroaryl replacements of the naphthalene. *Bioorg Med Chem Lett*. 2011; 21:1206–1213. [PubMed: 21256005]
- Bennett BJ, Farber CR, Orozco L, Min Kang H, Ghazalpour A, Siemers N, Neubauer M, Neuhaus I, Yordanova R, Guan B, Truong A, Yang WP, He A, Kayne P, Gargalovic P, Kirchgessner T, Pan C, Castellani LW, Kostem E, Furlotte N, Drake TA, Eskin E, Lusis AJ. A high-resolution association mapping panel for the dissection of complex traits in mice. *Genome Res*. 2010
- Bennett BJ, Orozco L, Kostem E, Erbilgin A, Dallinga M, Neuhaus I, Guan B, Wang X, Eskin E, Lusis AJ. High-resolution association mapping of atherosclerosis Loci in mice. *Arterioscler Thromb Vasc Biol*. 2012; 32:1790–1798. [PubMed: 22723443]
- Benson AK, Kelly SA, Legge R, Ma F, Low SJ, Kim J, Zhang M, Oh PL, Nehrenberg D, Hua K, Kachman SD, Moriyama EN, Walter J, Peterson DA, Pomp D. Individuality in gut microbiota composition is a complex polygenic trait shaped by multiple environmental and host genetic factors. *Proceedings of the National Academy of Sciences of the United States of America*. 2010; 107:18933–18938. [PubMed: 20937875]
- Bhattacharyya T, Nicholls SJ, Topol EJ, Zhang R, Yang X, Schmitt D, Fu X, Shao M, Brennan DM, Ellis SG, Brennan ML, Allayee H, Lusis AJ, Hazen SL. Relationship of paraoxonase 1 (PON1) gene polymorphisms and functional activity with systemic oxidative stress and cardiovascular risk. *Jama*. 2008; 299:1265–1276. [PubMed: 18349088]
- Cashman JR, Zhang J. Human flavin-containing monooxygenases. *Annu Rev Pharmacol Toxicol*. 2006; 46:65–100. [PubMed: 16402899]
- Chong HK, Infante AM, Seo YK, Jeon TI, Zhang Y, Edwards PA, Xie X, Osborne TF. Genome-wide interrogation of hepatic FXR reveals an asymmetric IR-1 motif and synergy with LRH-1. *Nucleic Acids Res*. 2010; 38:6007–6017. [PubMed: 20483916]

- Dumas ME, Barton RH, Toye A, Cloarec O, Blancher C, Rothwell A, Fearnside J, Tatoud R, Blanc V, Lindon JC, Mitchell SC, Holmes E, McCarthy MI, Scott J, Gauguier D, Nicholson JK. Metabolic profiling reveals a contribution of gut microbiota to fatty liver phenotype in insulin-resistant mice. *Proceedings of the National Academy of Sciences of the United States of America*. 2006; 103:12511–12516. [PubMed: 16895997]
- Ghazalpour A, Rau CD, Farber CR, Bennett BJ, Orozco LD, van Nas A, Pan C, Allayee H, Beaven SW, Civelek M, Davis RC, Drake TA, Friedman RA, Furlotte N, Hui ST, Jentsch JD, Kostem E, Kang HM, Kang EY, Joo JW, Korshunov VA, Laughlin RE, Martin LJ, Ohmen JD, Parks BW, Pellegrini M, Reue K, Smith DJ, Tetradis S, Wang J, Wang Y, Weiss JN, Kirchgessner T, Gargalovic PS, Eskin E, Lusis AJ, Leboeuf RC. Hybrid mouse diversity panel: a panel of inbred mouse strains suitable for analysis of complex genetic traits. *Mamm Genome*. 2012
- Hageman J, Herrema H, Groen AK, Kuipers F. A role of the bile salt receptor FXR in atherosclerosis. *Arterioscler Thromb Vasc Biol*. 2010; 30:1519–1528. [PubMed: 20631352]
- Hartman HB, Gardell SJ, Petucci CJ, Wang S, Krueger JA, Evans MJ. Activation of farnesoid X receptor prevents atherosclerotic lesion formation in LDLR^{-/-} and apoE^{-/-} mice. *J Lipid Res*. 2009; 50:1090–1100. [PubMed: 19174369]
- Kovacs A, Ben-Jacob N, Tayem H, Halperin E, Iraqi FA, Gophna U. Genotype is a stronger determinant than sex of the mouse gut microbiota. *Microbial ecology*. 2011; 61:423–428. [PubMed: 21181142]
- Lattard V, Zhang J, Cashman JR. Alternative processing events in human FMO genes. *Mol Pharmacol*. 2004; 65:1517–1525. [PubMed: 15155844]
- Lee FY, de Aguiar Vallim TQ, Chong HK, Zhang Y, Liu Y, Jones SA, Osborne TF, Edwards PA. Activation of the farnesoid X receptor provides protection against acetaminophen-induced hepatic toxicity. *Mol Endocrinol*. 2010; 24:1626–1636. [PubMed: 20573685]
- Lefebvre P, Cariou B, Lien F, Kuipers F, Staels B. Role of bile acids and bile acid receptors in metabolic regulation. *Physiol Rev*. 2009; 89:147–191. [PubMed: 19126757]
- Paigen B, Mitchell D, Reue K, Morrow A, Lusis AJ, LeBoeuf RC. Ath-1, a gene determining atherosclerosis susceptibility and high density lipoprotein levels in mice. *Proceedings of the National Academy of Sciences of the United States of America*. 1987; 84:3763–3767. [PubMed: 3473481]
- Ryu SD, Kang JH, Yi HG, Nahm CH, Park CS. Hepatic flavin-containing monooxygenase activity attenuated by cGMP-independent nitric oxide-mediated mRNA destabilization. *Biochem Biophys Res Commun*. 2004a; 324:409–416. [PubMed: 15465034]
- Ryu SD, Yi HG, Cha YN, Kang JH, Kang JS, Jeon YC, Park HK, Yu TM, Lee JN, Park CS. Flavin-containing monooxygenase activity can be inhibited by nitric oxide-mediated S-nitrosylation. *Life Sci*. 2004b; 75:2559–2572. [PubMed: 15363661]
- Schadt EE, Molony C, Chudin E, Hao K, Yang X, Lum PY, Kasarskis A, Zhang B, Wang S, Suver C, Zhu J, Millstein J, Sieberts S, Lamb J, GuhaThakurta D, Derry J, Storey JD, Avila-Campillo I, Kruger MJ, Johnson JM, Rohl CA, van Nas A, Mehrabian M, Drake TA, Lusis AJ, Smith RC, Guengerich FP, Strom SC, Schuetz E, Rushmore TH, Ulrich R. Mapping the genetic architecture of gene expression in human liver. *PLoS Biol*. 2008; 6:e107. [PubMed: 18462017]
- Shimizu M, Cashman JR, Yamazaki H. Transient trimethylaminuria related to menstruation. *BMC Med Genet*. 2007; 8:2. [PubMed: 17257434]
- Spencer MD, Zheng X, King SM, Xie G, Da Costa K-A, Fischer LM, Jia W, Zeisel SH. Menopause status explains large individual variation in cardiovascular disease risk marker response to different dietary choline intake levels. *The FASEB Journal*. 2012; 26:lb435.
- Thomas AM, Hart SN, Kong B, Fang J, Zhong XB, Guo GL. Genome-wide tissue-specific farnesoid X receptor binding in mouse liver and intestine. *Hepatology*. 2010; 51:1410–1419. [PubMed: 20091679]
- Touhara K, Vosshall LB. Sensing odorants and pheromones with chemosensory receptors. *Annu Rev Physiol*. 2009; 71:307–332. [PubMed: 19575682]
- Trapnell C, Pachter L, Salzberg SL. TopHat: discovering splice junctions with RNA-Seq. *Bioinformatics*. 2009; 25:1105–1111. [PubMed: 19289445]

- Treacy EP, Akerman BR, Chow LM, Youil R, Bibeau C, Lin J, Bruce AG, Knight M, Danks DM, Cashman JR, Forrest SM. Mutations of the flavin-containing monooxygenase gene (FMO3) cause trimethylaminuria, a defect in detoxication. *Human molecular genetics*. 1998; 7:839–845. [PubMed: 9536088]
- Turnbaugh PJ, Quince C, Faith JJ, McHardy AC, Yatsunencko T, Niazi F, Affourtit J, Egholm M, Henrissat B, Knight R, Gordon JI. Organismal, genetic, and transcriptional variation in the deeply sequenced gut microbiomes of identical twins. *Proceedings of the National Academy of Sciences of the United States of America*. 2010; 107:7503–7508. [PubMed: 20363958]
- Wang Z, Klipfell E, Bennett BJ, Koeth R, Levison BS, Dugar B, Feldstein AE, Britt EB, Fu X, Chung YM, Wu Y, Schauer P, Smith JD, Allayee H, Tang WH, DiDonato JA, Lusis AJ, Hazen SL. Gut flora metabolism of phosphatidylcholine promotes cardiovascular disease. *Nature*. 2011; 472:57–63. [PubMed: 21475195]
- Zeisel SH, daCosta KA, Youssef M, Hensey S. Conversion of dietary choline to trimethylamine and dimethylamine in rats: dose-response relationship. *J Nutr*. 1989; 119:800–804. [PubMed: 2723829]
- Zhang Y, Wang X, Vales C, Lee FY, Lee H, Lusis AJ, Edwards PA. FXR deficiency causes reduced atherosclerosis in *Ldlr*^{-/-} mice. *Arterioscler Thromb Vasc Biol*. 2006; 26:2316–2321. [PubMed: 16825595]

Highlights

- Hepatic FMO3 synthesizes TMAO from TMA.
- *In vivo* overexpression or silencing of FMO3 increases or decreases plasma TMAO levels, respectively.
- FMO3 expression is repressed by testosterone and induced by bile acids via the nuclear receptor FXR.
- Natural variations of TMAO levels in mice contributes to atherosclerosis susceptibility.

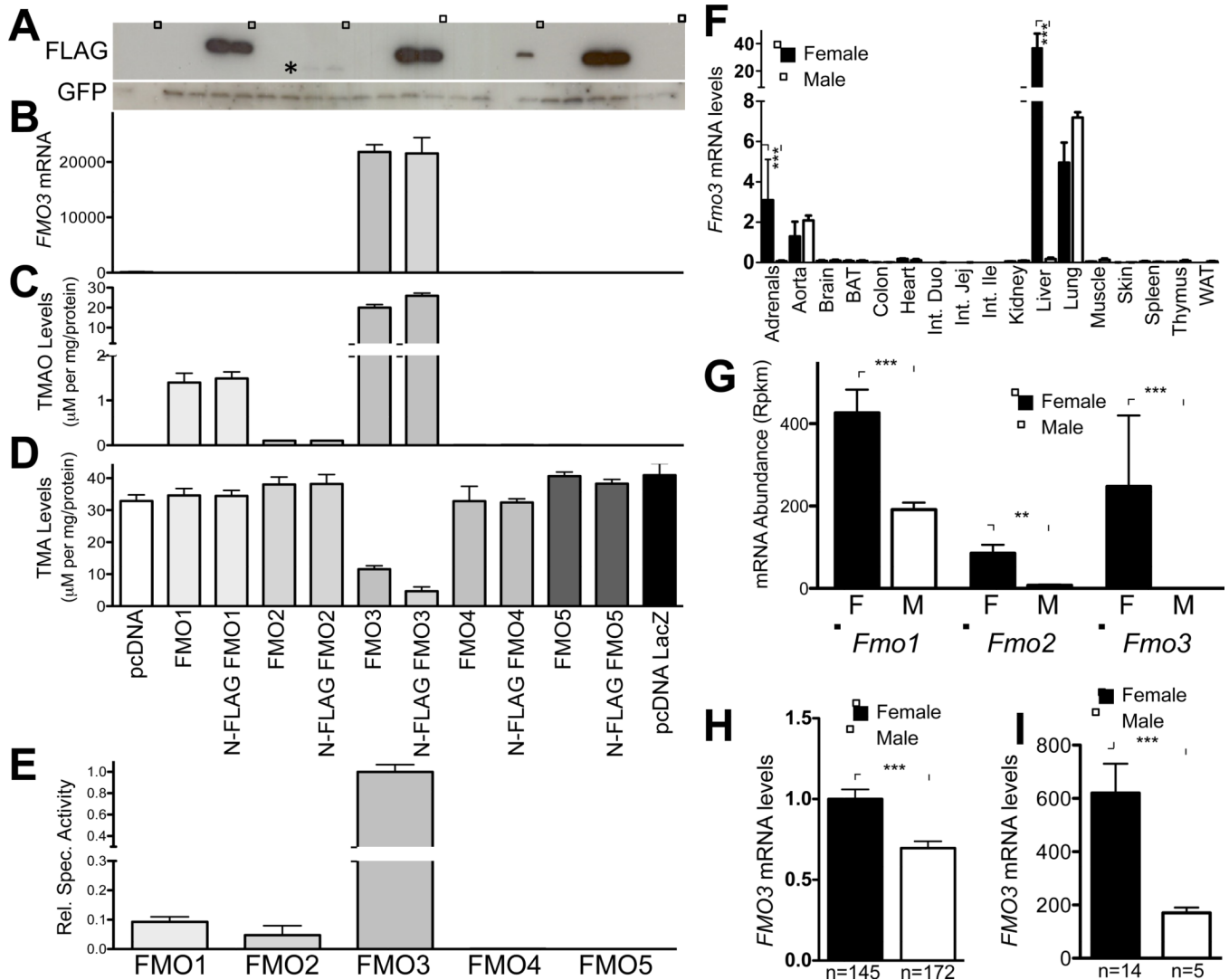


Figure 1. FMO3 is the Major FMO Family Member Responsible for the Conversion of TMA to TMAO

(A–D) Overexpression of untagged or FLAG-tagged human FMO1–5 in HEK292Ad cells. (A) Western blotting analysis of FLAG-tagged FMO1–5 transfected into HEK293Ad cells. GFP was co-transfected to normalize transfection efficiency. (B) FMO3 mRNA levels were determined by RT-qPCR and normalized to GFP mRNA levels. (C and D) TMAO and TMA levels determined in the media of transfected cells treated with d9-TMA and then analyzed for d9-TMA and d9-TMAO levels using mass spectrometry (see Experimental Procedures). TMAO production was determined from triplicate wells for each condition and normalized to the amount of protein per well. (E) Relative specific activity of FMO1–5 determined by dividing normalized TMAO levels by relative FMO protein levels calculated by densitometry analysis and expressed relative to FLAG-FMO3 activity. (F) Relative *Fmo3* mRNA levels in various mouse tissues from C57BL/6 mice (n=3 mice/sex). Expression was determined by RT-qPCR and was normalized to 36B4 expression levels. (G) Relative abundance of FMO1–3 determined by RNA-Seq analysis from male and female C57BL/6 mice. (H) Relative FMO3 expression in human liver determined by microarray expression profile from 317 Caucasian human individuals segregated by sex. (I) RT-qPCR analysis of hepatic mRNA levels from human liver biopsies obtained as described in Experimental

Procedures. Data are presented as mean \pm SEM. Significance was measured with Student's t-test. * indicates $p < 0.05$ and *** indicates $p < 0.001$.

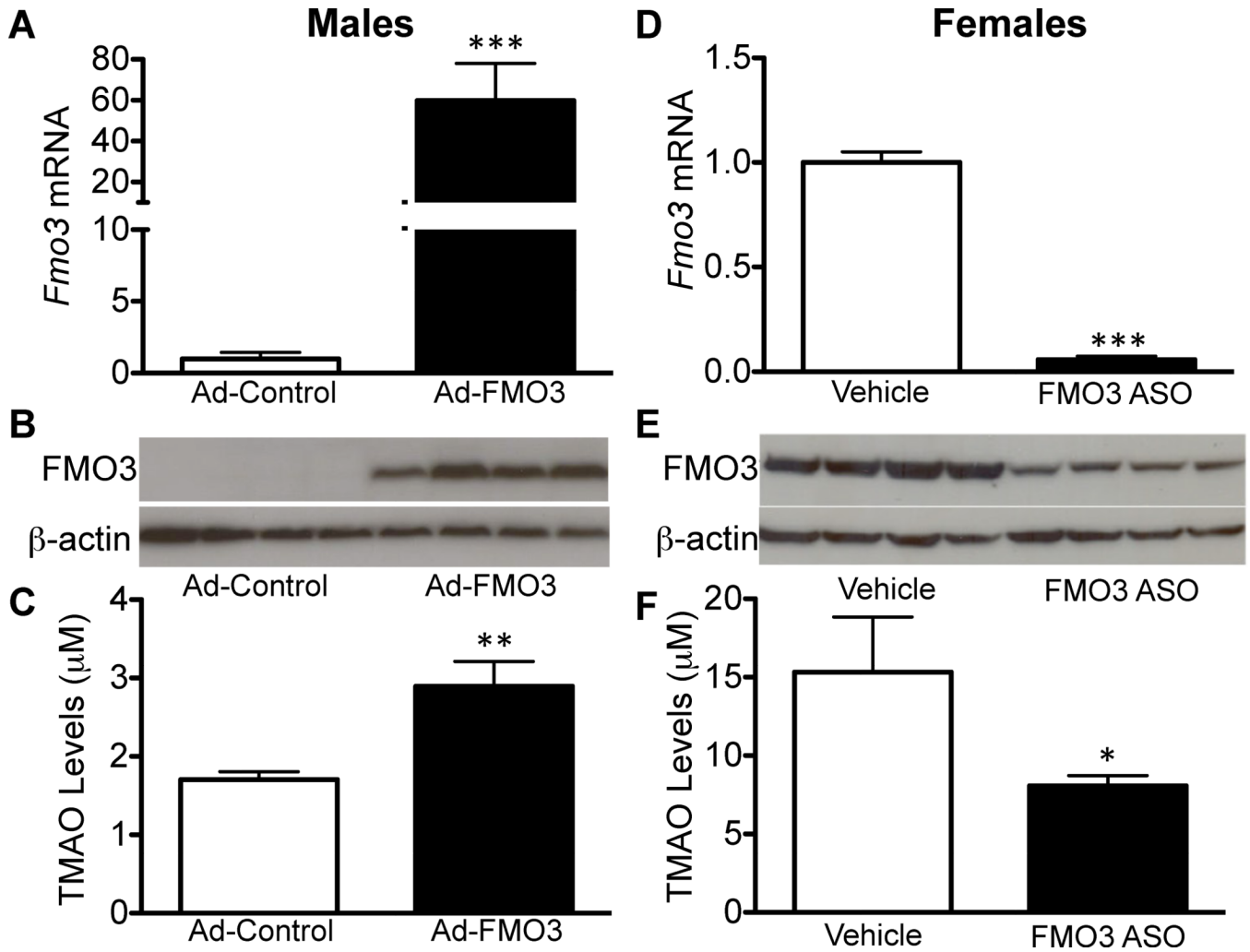


Figure 2. Modulation of Hepatic FMO3 levels in Mice Regulates Plasma TMAO Levels (A–C) FMO3 overexpression in the livers of male C57BL/6 mice infected with either Ad-control or Ad-FMO3 for 7 days (n=8 mice/group). (D–F) FMO3 knockdown in livers of female C57BL/6 mice treated with either vehicle (saline) or FMO3 antisense oligonucleotide (ASO) once weekly (50mg/kg body weight) for 7 weeks (n=4 mice/group). (A, D) Hepatic FMO3 mRNA levels determined by RT-qPCR and normalized to 36B4 or cyclophilin levels. (B, E) Hepatic FMO3 protein levels determined by Western blotting analysis normalized to β -Actin levels. (C, E) Plasma TMAO levels determined from plasma isolated from adenovirus-treated or ASO- or vehicle-treated mice. TMAO levels were determined by LC/MS/MS.

Data are presented as mean \pm SEM. Significance was measured with Student's t-test. * indicates $p < 0.05$, ** indicates $p < 0.01$ and *** indicates $p < 0.001$.

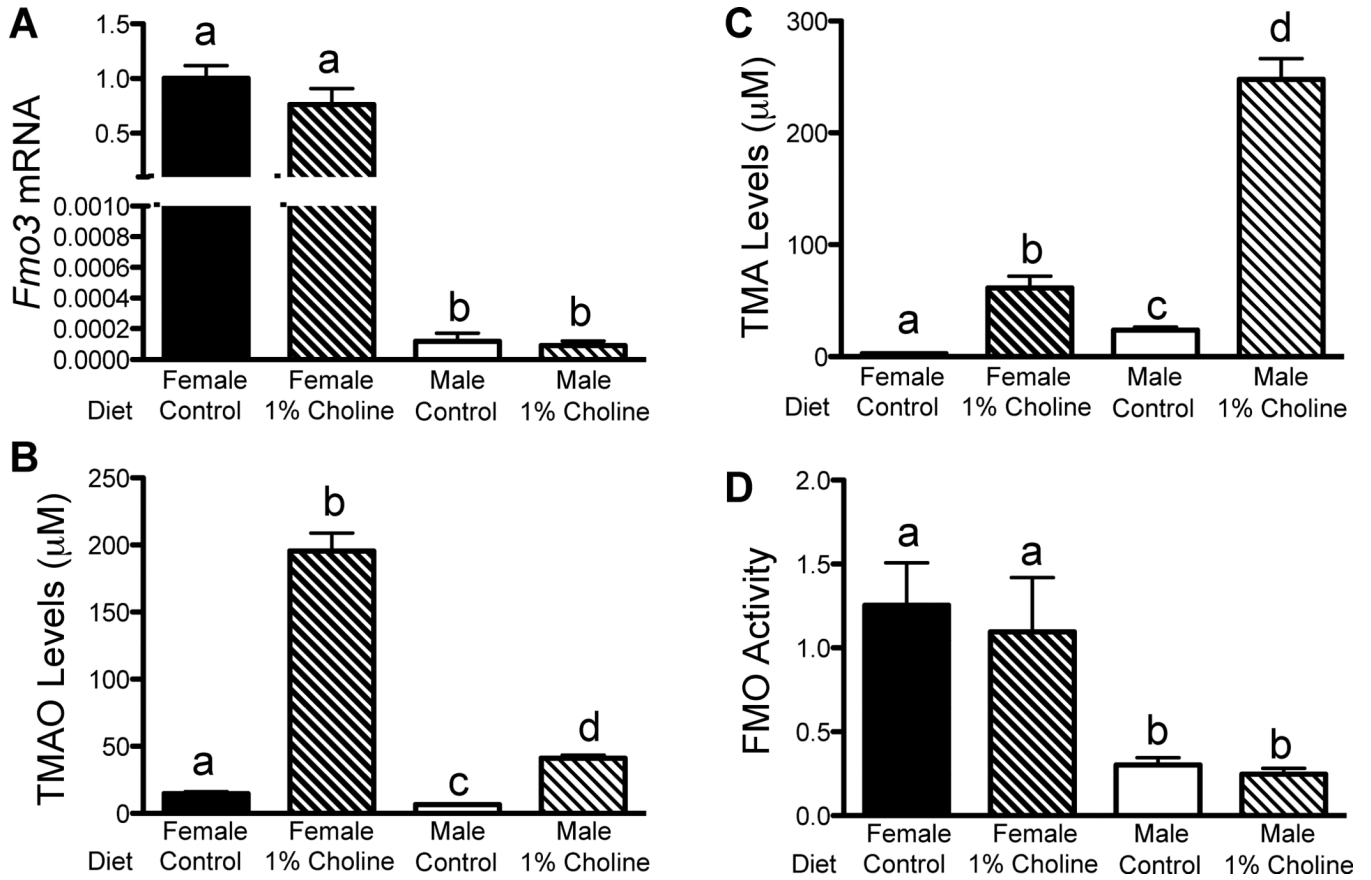


Figure 3. Sex and Dietary Choline Regulate Hepatic FMO3 Expression and Plasma TMAO Levels in Mice

(A–D) Male and female *ApoE*^{-/-} mice were fed either a control (chow) or choline-rich diet (1% choline) (n=7–10 mice/group). (A) Hepatic *Fmo3* mRNA levels determined by RT-qPCR and normalized to 36B4 expression. (B) Plasma TMAO and (C) TMA levels from male and female mice determined by LC/MS/MS. (D) Conversion of TMA into TMAO by liver homogenates (FMO activity) of male and female mice normalized to total hepatic protein levels. Data are presented as mean \pm SEM. Significance was measured with One-way ANOVA and different letters (a–d) indicate statistically significant (p<0.05 or greater) differences between groups.

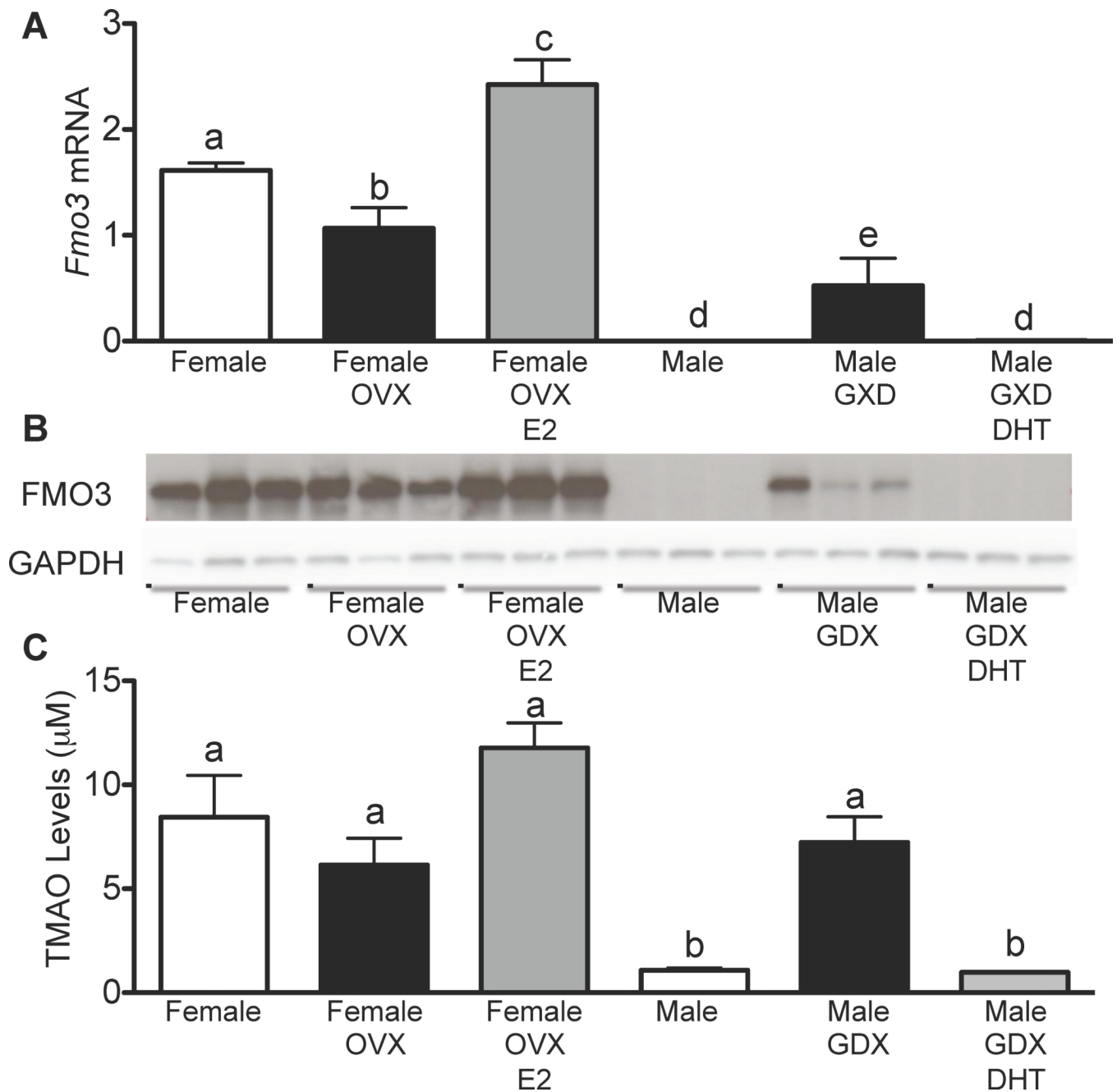


Figure 4. Gonadal Hormones Regulate Hepatic FMO3 Expression and Plasma TMAO Levels (A–C) Male and female C57BL/6 mice were either untreated or gonadectomized or ovariectomized and then treated with vehicle or DHT (males) or estrogen (females) (n=4–6 mice/group). (A) Hepatic FMO3 expression was determined by RT-qPCR and normalized to 36B4. (B) FMO3 protein levels were determined by Western blot analysis and GAPDH was used as a control. (C) Plasma TMAO levels from male and female mice were determined by LC/MS/MS. Data are presented as mean ± SEM. Significance was measured with One-way ANOVA and different letters (a–e) indicate statistically significant ($p < 0.05$ or greater) differences between groups.

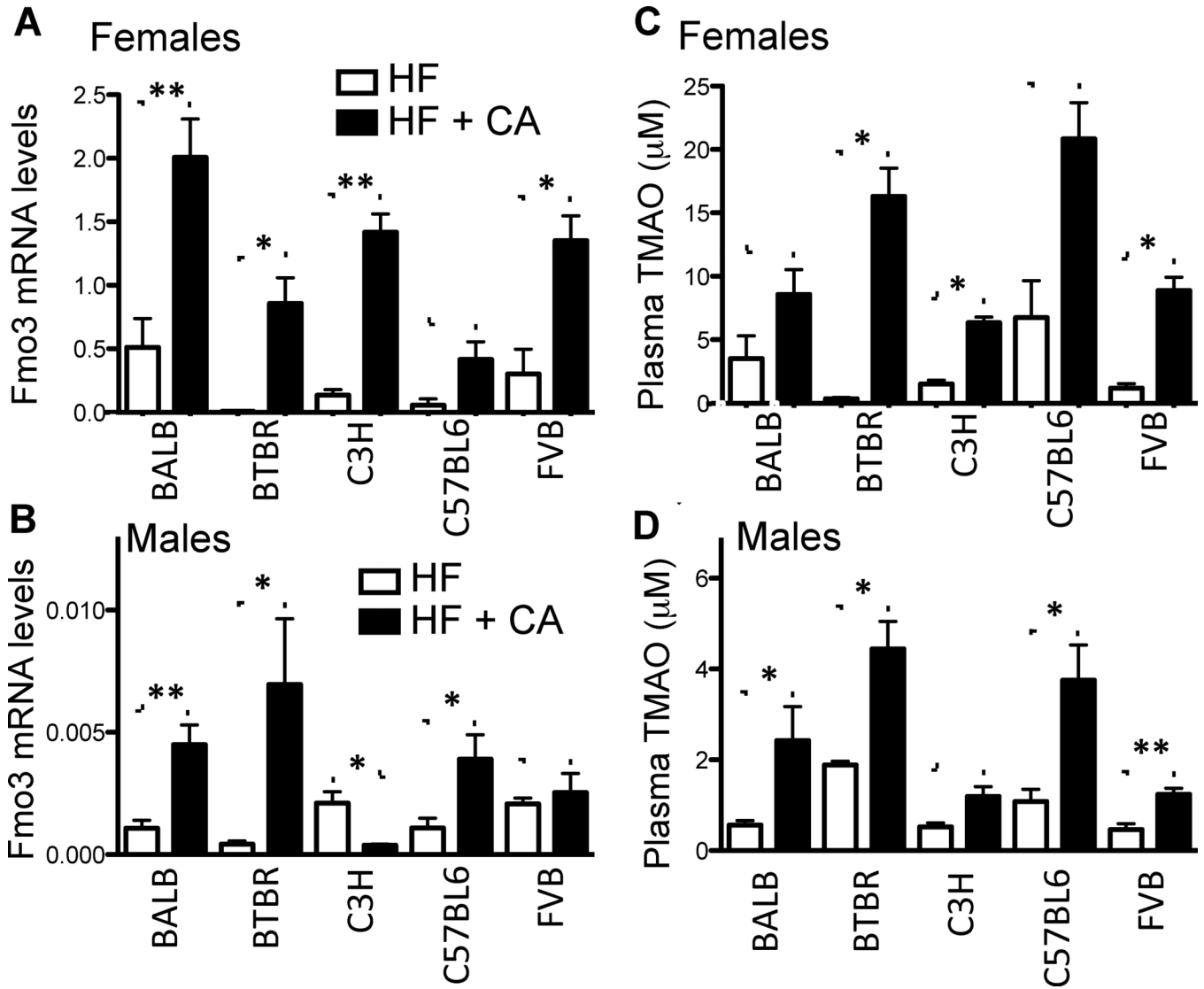


Figure 5. Dietary Cholic Acid Induces *Fmo3* Expression and TMAO Levels in Common Inbred Mouse Strains

Female (A, C) and male (B, D) “humanized” ApoB100 transgenic mice were fed a high fat diet with cholic acid (HF+CA) or without cholic acid (HF) (n=2–9 mice/strain/gender). (A, B) Hepatic FMO3 expression was determined by RT-qPCR normalized to 36B4 expression. (C, D) Plasma TMAO levels from male and female mice of different strains were determined by LC/MS/MS. Data are presented as mean ± SEM. Significance was measured with Student’s t-test. *indicates p < 0.05, ** indicates p < 0.01 and *** indicates p < 0.001.

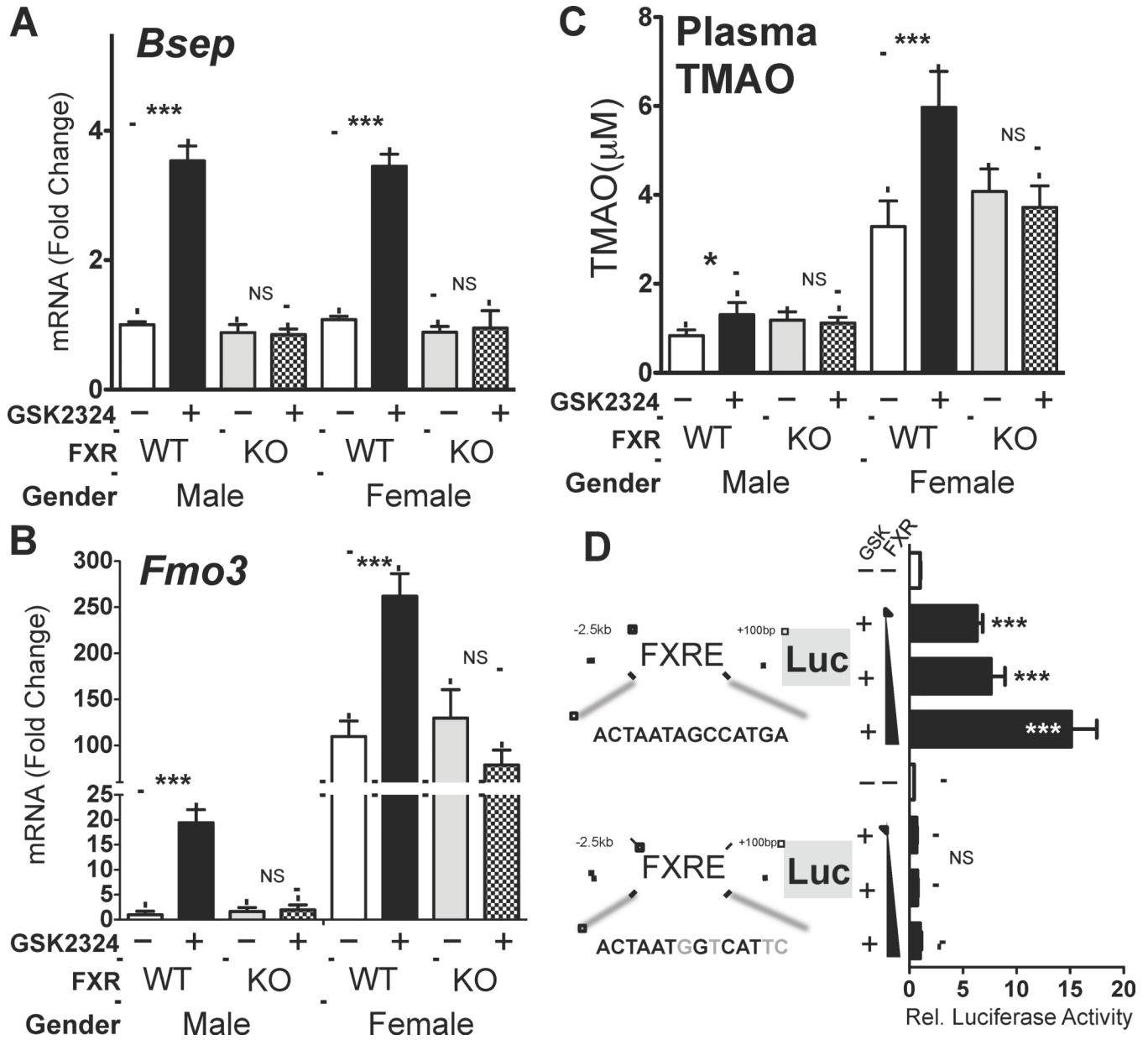


Figure 6. FMO3 is an FXR Target Gene and FXR Activation Induces FMO3 and Increases Circulating TMAO Levels *in vivo*
 (A) Hepatic *Bsep* and (B) *Fmo3* mRNA levels normalized to 36B4, were determined in male and female wild-type and *Fxr*^{-/-} mice treated with GSK2324 at 30 mpk/day for 3 days (n=7–10 mice/group). (C) Plasma TMAO levels from the same mice were determined by LC/MS/MS. (D) Luciferase reporter plasmids under the control of either 2.5kb of the wild type mouse FMO3 promoter or the promoter containing a mutant FXRE, were transfected into Hep3B cells (6 wells per condition) in the presence of increasing amounts of pcDNA FXR 2 and treated with vehicle (water) or GSK2324 (1 μM). Promoter activity was determined by luciferase assay and normalized to β -galactosidase (co-transfected to account for transfection efficiency). Data are presented as mean \pm SEM. Significance was measured with Student's t-test. * indicates p < 0.05, ** indicates p < 0.01 and *** indicates p < 0.001.

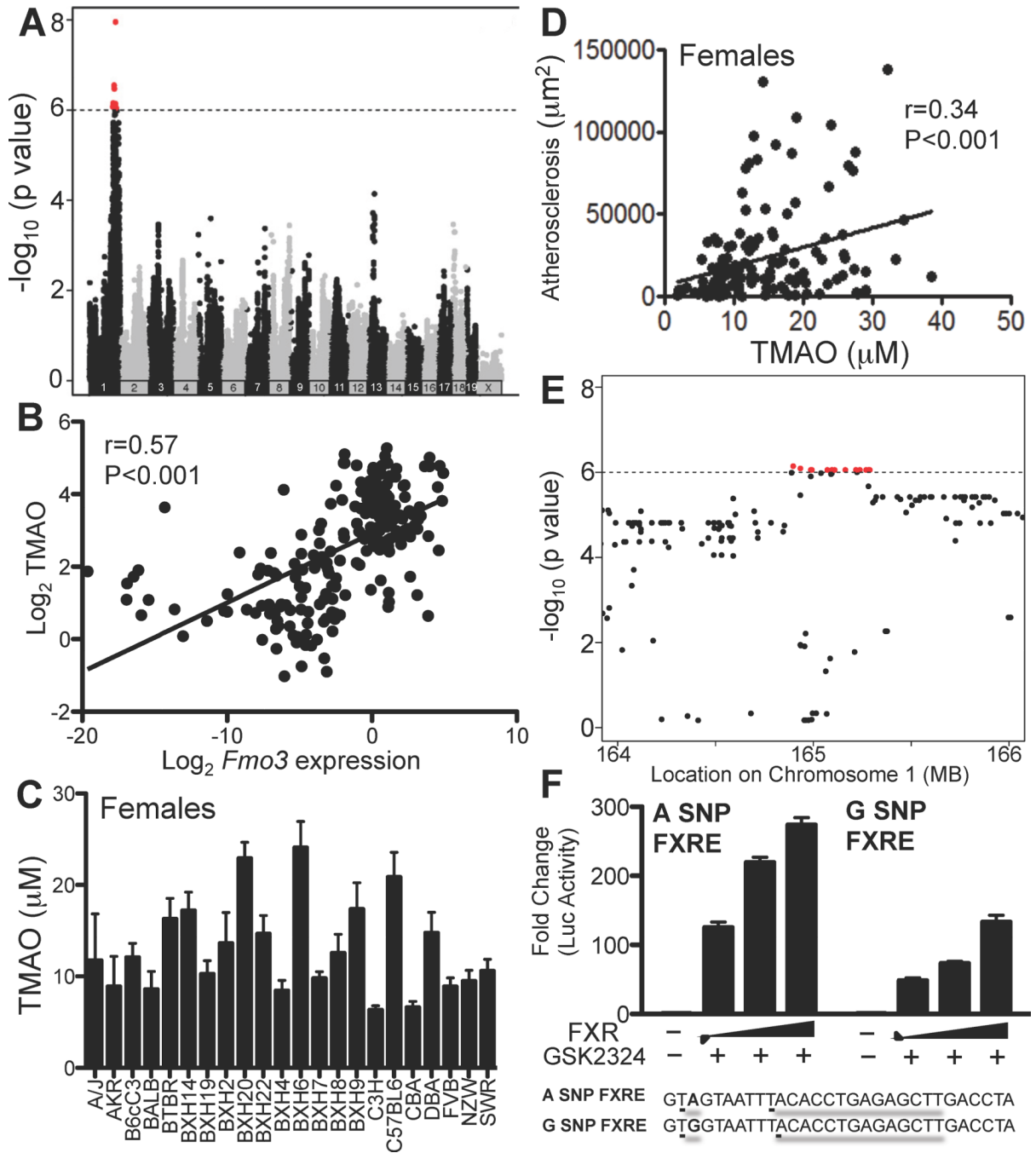


Figure 7. Natural Genetic Variation of Hepatic FMO3, Plasma TMAO Levels and Atherosclerosis among Common Inbred Strains of Mice

(A) Identification of a *cis*-acting expression Quantitative Trait Locus (eQTL) for FMO3 among the 100 HMDP strains of mice. Approximately 135,000 SNPs varying across the HMDP panel were examined for association with FMO3 transcript levels following correction for population structure (see Experimental Procedures). The location of each SNP across the 19 autosomes and the X chromosome is indicated on the X-axis and the strength of association is shown on the Y-axis. Signals shown in red indicate genome-wide significant results. (B) Relationship between hepatic FMO3 transcript levels and circulating TMAO levels in 22 strains (males and females) carrying the human ApoB transgene fed a

Western diet. (C) TMAO levels in female mice of the 22 hyperlipidemic strains on a Western diet. (D) Relationship between atherosclerotic lesions and TMAO levels in female mice of the 22 hyperlipidemic strains (points represent single animals). Atherosclerotic lesions were quantitated following the sectioning of the aortic sinus and proximal aorta. (E) A high-resolution image of panel A showing that the peak SNPs reside over the location of the FMO3 gene on Chromosome 1. (F) Three copies of the DNA region containing the A or G SNP adjacent to the intergenic FXRE were cloned into a minimal TK promoter luciferase reporter plasmid. SNP reporter plasmids were transfected into Hep3B cells (6 wells/condition) with increasing amounts of pcDNA FXR 2 and treated with vehicle (water) or GSK2324 (1 μ M). Promoter activity was determined by luciferase assay and normalized to -galactosidase (co-transfected to account for transfection efficiency). Data are presented as mean \pm SEM.